49th AIAA Aerospace Sciences Meeting including the New Horizons Forum and Aerospace Exposition
4 - 7 January 2011, Orlando, Florida

AIAA 2011-880

49th AIAA Aerospace Science Meeting, Orlando, FL USA, 4-7 January 2011

Hot-Wire Measurements in Cryogenic Environment

Harald Quix[1], Jürgen Quest[2] and Christian Brzek[3]
European Transonic Windtunnel GmbH, 51147 Cologne, Germany

The hotwire anemometry is a well known measurement technique used in several applications to determine flow velocity and to investigate flow quality. Using this measurement technique in a cryogenic environment is not very common and therefore the knowledge about it is very limited. The European Transonic Windtunnel, as cryogenic high Reynolds number test facility, is establishing the hotwire measurement technique to support flow quality measurements required by future laminar flow test campaigns. The present paper describes the challenges of such a system setup in ETW, its application and presents first results gathered in the pilot facility of the European Transonic Windtunnel. Thereby the main objective of this paper is to give a general overview about the first achieved results and to discuss the different influencing parameters on the hotwire output signal over the complete operational envelope of ETW/PETW.

Nomenclature

E_{br}	anemometer bridge voltage	[V]
E_w	hotwire voltage	[V]
h	heat transfer coefficient	$[\mathrm{W/(m^2K)}]$
k	thermal conductivity	$[\mathrm{W/(Km)}]$
Nu	Nusselt number	[-]
P_{tot}	total pressure	[Pa]
P_{stat}	static pressure	[Pa]
Re	Reynolds number	[-]
R_c	cable resistance	$[\Omega]$
R_{fix}	fixed resistance	$[\Omega]$
R_o	overheat setup resistance	$[\Omega]$
R_{sup}	support resistance	$[\Omega]$
R_w	wire resistance	$[\Omega]$
T_{tot}	total temperature	[K]
T_{stat}	static temperature	[K]
Tu	turbulence level	[-]
U_{flow}	tunnel flow velocity	[m/s]
U	flow velocity perpendicular to wire	[m/s]
$\overline{U}$	mean flow velocity	[m/s]
$\widetilde{u}, \widetilde{v}, \widetilde{w}$	velocity fluctuations	[m/s]
T_{rec}	recovery temperature	[K]
ρ	density	$[\mathrm{kg/m^3}]$
γ	overheat ratio	[-]

[1]Aerodynamic and Data Processing Engineer, AIAA member
[2]Chief Aerodynamicist, AIAA associated fellow
[3]Research assistant

Copyright ' 2011 by the author(s). Published by the American Institute of Aeronautics and Astronautics, Inc., with permission.

I. Introduction

The hotwire anemometry has now been used for several decades in the field of aerodynamic research. Based on the principle of heat transfer, it is the only measurement technique providing a direct link between the physical measurement variable and the output signal. Therefore and because of its capability to measure highly dynamic phenomena, its simple setup and its general applicability for gaseous flows, it is still widely used as research tool in fluid mechanics. For standard applications at ambient pressure, ambient temperature and subsonic speeds, the hotwire anemometry technique is very well documented and a lot of results are available. But leaving these standard conditions in any direction by changing pressure, temperature or going to transonic speeds, the available literature is diminished and the system setup and result analysis becomes more and more challenging. The present paper discusses the application of hotwire anemometry under the cryogenic conditions of the European Transonic Windtunnel (ETW). ETW is the world leading High-Reynolds number testing facility and unique with respect to the performance of natural laminar flow investigations at flight Reynolds numbers. To support the analysis of laminar test data the knowledge about individual turbulence levels of the flow is essential. Hence, it is considered mandatory establishing the hotwire technique for a reliable application under cryogenic test conditions in ETW to perform relevant turbulence measurements. First trials to gain experience on this subject have already be made by Dr. Michel from DLR in the mid of the ninetees and ONERA a few years ago but without being comprehensive. Now, in the light of a worldwide increasing interest in laminar wings a new approach has beeen initiated. Tests were performed in the pilot facility (PETW) of the European Transonic Wind (ETW) tunnel, which has the same operational envelope as ETW, but is more cost efficient for development of new measurement techniques due to its smaller size (scaled down from ETW by 1:8.8). Based on the special capabilities of ETW and PETW, allowing separating between compressibility, friction and deformation effects, it is possible to investigate the influence of different parameters on the heat transfer of a hotwire, offering a better chance for reaching a comprehensive understanding of the hotwire behavior. This is necessary for an application of the technique in future tests, where different relevant parameters may change simultaneously. Hence, the goal is to find an approach allowing a complete correction of disturbing effects and, hence, expanding the knowledge about hotwire measurements.
The present paper shortly describes the basic hotwire principle, explains the test facilities and the test setup before discussing results gathered in PETW. These first results show basic relations between hotwire output and variable tunnel conditions, but with respect to the complexity of the subject and the amount of gathered steady and unsteady data will not provide final conclusions regarding the application of hotwires under cryogenic conditions. This will be given in a follow on paper.

II. Hotwire Anemometry

The general hardware setup of hotwire measurements is quite simple. It consists of the hotwire probe and the anemometer unit. The hotwire sensor itself is a very thin wire (about 5 -20 microns diameter)with a small length which is exposed to the wind tunnel flow. Single, double and triple wire probes are common. Fig. 1 shows a Dantec shortcut probe and a Dantec double probe, called x-wire probe as being used in the described investigations.

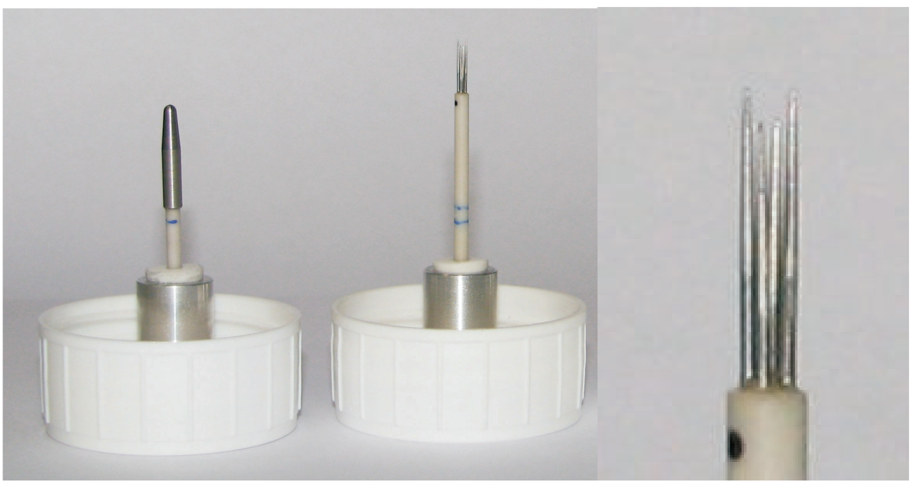

Fig. 1. DANTEC shortcut probe (left) and x-wire sensor (right and zoom)

The anemometer is the electrical circuit containing a Wheatstone bridge and a power controller able keeping the hotwire sensor at a constant resistance and therewith at a constant temperature. Alternative anemometer setups exist, like the constant current anemometer (CCA) or the constant voltage (CVA), but the present paper focuses on the constant temperature anemometer (CTA) setup which holds the longest tradition in application. The basic principle behind the hotwire measurement technique is the heat transfer caused by forced convection. At ambient low speed conditions the heat transfer from the heated wire to the surrounding flow is mainly a function of flow velocity, but especially for cryogenic and pressurized facilities like ETW and PETW additional variables are going affecting it.

The heat transfer is changing with varying flow parameters causing the hotwire resistance to change by cooling down the wire. This leads obviously to an unbalanced Wheatstone bridge by a difference in the voltages E1 and E2 (Fig. 8) of the two bridge branches. This difference is measured by the operational amplifier C controlling the bridge current to maintain its balance. Consequently, the bridge voltage would change, but such a reaction is avoided by the fast electrical circuit of the anemometer. The anemometer provides a controlled amount of current to keep the hotwire resistance and therewith also the temperature of the wire itself at a constant value. Effectively, the voltage of the Wheatstone bridge responds to the changes of the heat transfer at the hotwire, representing a direct link between the physical phenomena and the analog output signal. So, the electrical power provided by the electrical circuit is directly proportional to the heat loss at the wire. The electrical power is defined by:

$$Q_{el} = R_w \cdot I_w^2 = \frac{E_w^2}{R_w} \tag{1}$$

To determine the electrical power the wire voltage has to be extracted from the bridge voltage using the following correlation:

$$E_w = E_{br} \cdot \frac{R_w}{R_w + R_c + R_{sup} + R_{fix}} \tag{2}$$

Using this equation at different temperature levels, it is important to keep in mind that the wire resistance R_w as well as the cable and support resistances, R_c and R_{sup} are linearly depending on temperature. The wire resistance R_w and therewith the wire temperature is defined by the overheat ratio, which is the ratio between the resistance of the heated wire and its unheated state:

$$\gamma = \frac{R_{w_{hot}}}{R_{w_{cold}}} \tag{3}$$

This overheat ration is set by the resistance R_0 which defines also the wire resistance R_w in a balanced bridge. Typically, overheat ratios are selected between 1.6 and 2.2, in most cases a value of 1.8 is used. In the described investigations a overheat ratio of $\gamma = 2[-]$ is used for most of the test cases, to increase the wire sensitivity.
The previous equations describe the electrical power which can ideally be directly linked to the heat loss at the wire. The heat transfer from hotwire to the surrounding flow is depending on different kinds of heat losses, like heat radiation, heat conduction and heat convection as well as on heat losses to the prongs of the hotwire probe. As higher flow velocities as well as long wires (L/d>200) are considered the forced convection losses are dominant, allowing a neglection of all other losses, resulting in the following equation:

$$Q_{el} = Q_{conv} \tag{4}$$

The heat loss by forced convection is defined by:

$$Q_{conv} = A_w \cdot h \cdot (T_w - T_{tot}) \tag{5}$$

with

$$h = f(U, \rho, T_w) \tag{6}$$

Often you will find the recovery temperature or the film temperature to be used instead of T_{tot} in equation (5). Because h is depending on several parameters it is difficult to be determined accurately and therefore often unknown.

To overcome this problem the dimensionless Nusselt number is widely used. The Nusselt number describes the relation between heat transfer and heat radiation as:

$$Nu = \frac{h \cdot d}{k} \tag{7}$$

with

$$Nu = f(Re, Pr, Ma, ...) \tag{8}$$

Substituting h in equation (5) by the Nusselt number and taking into account equation (4) gives a direct link between the anemometer bridge output and the Nusselt number:

$$E_{br}^2 \cdot \frac{R_w}{(R_w + R_c + R_{sup} + R_{fix})^2} = \frac{E_w^2}{R_w} = A_w \cdot \frac{Nu \cdot k}{d} \cdot (T_w - T_{tot}) = \pi \cdot l \cdot k \cdot Nu \cdot (T_w - T_{tot}) \tag{9}$$

The Nusselt number itself is also depending on several parameters, but mainly influenced by Reynolds and Prandtl number. Many investigations were performed to determine a universal law to describe the cooling of a cylinder in flow, resulting in different equations for different Reynolds number ranges, which can be compared to the results of the hotwire measurement, because according to equation (9) it is possible to extract the Nusselt number from anemometer output voltage and therewith to determine the relation to the Reynolds number, Prandtl number and other influence parameters.

$$Nu = \frac{E_w^2}{R_w} \cdot \frac{1}{\pi \cdot l \cdot k \cdot (T_w - T_{tot})} = E_{br}^2 \cdot \frac{R_w}{(R_w + R_c + R_{sup} + R_{fix})^2} \cdot \frac{1}{\pi \cdot l \cdot k \cdot (T_w - T_{tot})} \tag{10}$$

To identify the different influence parameters on the hotwire output and therewith on the Nusselt number, a calibration of the hotwire is necessary. Thereby the goal is to separate the influencing parameters by changing only one at a time while keeping the others constant. For example, changing the flow velocity by keeping the other parameters constant results in a known dependency between bridge output and velocity following the King's law:

$$E_{br}^2 = A + B \cdot U^n \tag{11}$$

where A and B are constants. A is representing the free convection of the heated wire at zero velocity, while B indicates the sensitivity of the hotwire. The King's law by using bridge voltage and velocity has its analogon by using the Nusselt and the Reynolds number:

$$Nu^2 = C + D \cdot Re^n \tag{12}$$

C and D are also constants but not naturally equal to A and B.
The variation of other parameters like density and temperature in a cryogenic wind tunnel may show, whether and how the King's law has to be adapted or modified to cope the different influences.

Turbulence Measurements

Because the flow velocity in ETW/PETW is well known from the tunnel calibration, the main purpose of future hotwire measurements is the determination of the turbulence level.
For the dynamic response it is generally assumed that it is equal to the static response and the static calibration therefore is valid for the dynamic sensitivity as well. Although the static calibration may separate the different influence parameters this is not easily achievable for the dynamic case. Here, the hotwire signal is sensitive to all three basic fluctuation fields in the tunnel, notably velocity, density and temperature:

$$dE = \left(\frac{\partial E}{\partial U}\right)_{\rho, T=const} \cdot dU + \left(\frac{\partial E}{\partial \rho}\right)_{T, U=const} \cdot d\rho + \left(\frac{\partial E}{\partial T}\right)_{U, \rho=const} \cdot dT \tag{13}$$

Because theoretically all fluctuation fields exist simultaneously it is very demanding to separate them. Relevant ways may be to apply different overheating ratios (assessing temperature fluctuations) when applying the CTA method or going for the CCA method as used by Russian research Institute ITAM in Novosibirsk. Therefore, in a first approach the calculated turbulence level will contain at least the density and velocity fluctuations, while the temperature fluctuations can be neglected for high overheat ratios, where the wire temperature is large compared to the flow temperature. Nevertheless, in this first approach it will be assumed all fluctuations to be pure velocity fluctuations only. Further analysis and separation of the different fluctuation fields will be part of future experimental and analytical work. With this assumption the turbulence level is defined as:

$$Tu = \frac{\widetilde{U}}{\overline{\overline{U}}} \tag{14}$$

with

$$\widetilde{U} = \sqrt{\frac{1}{3} \cdot (\widetilde{u}^2 + \widetilde{v}^2 + \widetilde{w}^2)} \tag{15}$$

By using an x-wire probe with two wires inclined by 45 degree to the mean flow direction, it is possible to measure velocity fluctuations in two dimensions. Each wire measures the parts $\widetilde{u}$ and $\widetilde{v}$, so that it is possible to separate them by using both wire signals:

$$Tu_x = \frac{\widetilde{u}}{\overline{\overline{U}}} = \frac{1}{2} \cdot ((\frac{\widetilde{u}}{\overline{\overline{U}}})_{w1} + (\frac{\widetilde{u}}{\overline{\overline{U}}})_{w2})) \tag{16}$$

$$Tu_y = \frac{\widetilde{v}}{\overline{\overline{U}}} = \frac{1}{2} \cdot ((\frac{\widetilde{v}}{\overline{\overline{U}}})_{w1} - (\frac{\widetilde{v}}{\overline{\overline{U}}})_{w2})) \tag{17}$$

Assuming that missing turbulence level Tu_z of the third dimension is in the same magnitude as Tu_y, it is possible to calculate the overall turbulence level of the wind tunnel from the two-dimensional x-wire probe.

$$Tu = \sqrt{\frac{1}{3} \cdot (Tu_x^2 + Tu_y^2 + Tu_z^2)} = \sqrt{\frac{1}{3} \cdot (Tu_x^2 + 2 \cdot Tu_y^2)} \tag{18}$$

III. Test Facilities

A. European Transonic Windtunnel (ETW)

ETW is the most advanced aerodynamic test facility in the world. By applying low temperature operation, ETW is capable of accurately simulating actual high-lift and high-speed flight conditions of modern transport aircraft, defined by the Mach number and the Reynolds number. Fundamentally, if the temperature of the flow is decreased, the viscosity of the gas and the speed of sound decrease and the density will raise. Hence, the overall effect of cooling is a rapid increase of the Reynolds number. Thus, a pressurized tunnel at very low "cryogenic" temperatures can provide real-flight Reynolds numbers by virtue of both increased pressure and decreased temperature. A remarkable advantage of the cryogenic concept applied to a pressurized tunnel is that Mach number, Reynolds number and dynamic pressure can be varied independently, thus, keeping the others constant allowing studies of their individual effects (i.e. compressibility, friction and deformation). In ETW the models are not tested in an air environment, as in conventional wind tunnels. Instead, a pure nitrogen flow with temperatures down to 110 Kelvin is generated across the closed aerodynamic circuit (Fig. 2) of the wind tunnel, subjected to pressures up to 4.5 bars and passing the test section (2.0 m 2.4 m) at speeds form the low subsonic range (M = 0.15) up to the low supersonic range (M = 1.35). With its exceptional characteristics combined with a extremely good flow quality ETW is unique and the only aerodynamic facility able to perform natural laminar flow investigations under real-flight Reynolds numbers. Therewith the facility is essential for the development of upcoming steps in future aircraft design.

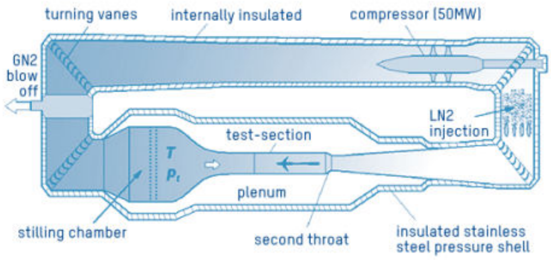

Fig. 2. ETW aerodynamic circuit

Fig. 3. Full model in ETW test section

B. Pilot European Transonic Windtunnel (PETW)

The Pilot European Transonic Windtunnel (PETW) has the same unique characteristics as the ETW, but is scaled down by 1:8.8 compared to ETW. Originally, PETW has been built as a test facility to validate the cryogenic wind tunnel technology in a small facility before going for the final design of ETW. Fig. 4 shows a schematic sketch of the PETW. Although ETW is mechanically not just a bigger copy of PETW both tunnels cover exactly the same Mach number, temperature and pressure range. The main differences between the tunnels are the setpoint control, which is manual in PETW resulting in a lower accuracy and stability, and the type of insulation (PETW features an external insulation of a box type while ETW is fully internally insulated).
PETW's main advantage is its much lower power and nitrogen consumption and its good accessibility of the test section (Fig 5). Summarizing, the Pilot European Transonic Windtunnel represents all famous flow characteristics of ETW, lower costs and a good accessibility and is therefore ideally qualified for the development and validation of new measurement techniques before introducing them in ETW.

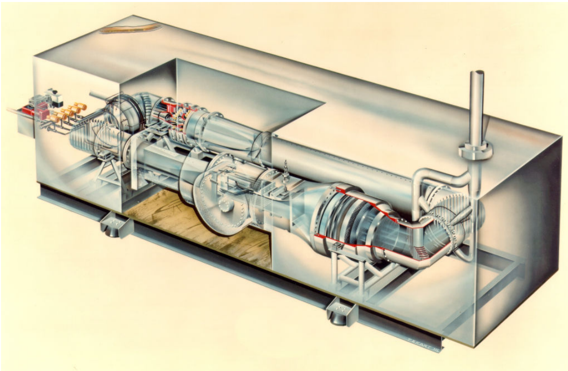

Fig. 4. Schematic sketch of PETW

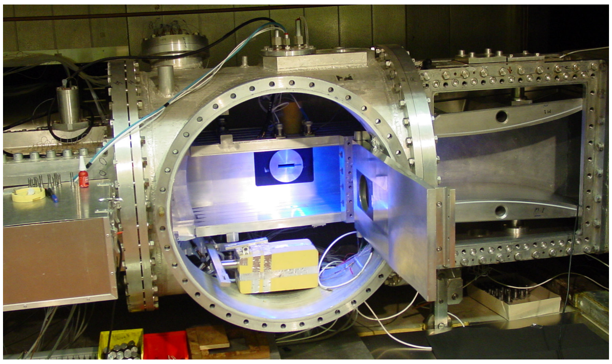

Fig. 5. PETW with open test section

IV. Test Setup

For the use in ETW the standard hotwire anemometry setup has to be adapted to the special requirements of a cryogenic test facility. The wide temperature range between 110 K and 300 K is the most obvious difference to conventional wind tunnels. This temperature difference results in some related aspects which have to be taken into account. One of the most challenging aspect is the long distance between the test section under cryogenic conditions and the measurement cabin at ambient temperature. Fig. 6 displays the arrangement of ETW's movable model cart and shows the temperature barrier between cryogenic part and the ambient part.

This distance requires 25 meters of cryo suitable cables. For this purpose a CAT-5 cable was successfully validated under cryogenic conditions. The cable has 4 twisted pairs of wire, hence, exactly matching the required number. Two pairs are required for the chosen double hotwire probe and the two other pairs are necessary to compensate for the changing cable resistance as a function of temperature. Because the cable passes the tunnel isolation from the cryogenic temperature side to the instrumentation cabin at ambient temperature, the wires subject to a floating resistance, requiring a real time compensation of it to get reasonable results. Therefore, the two additional wire pairs are compensation wires shortcutted at their ends using a Dantec shortcut probe. This setup ensures an automatic cancellation of temperature changes of the cabling by the anemometer bridge.

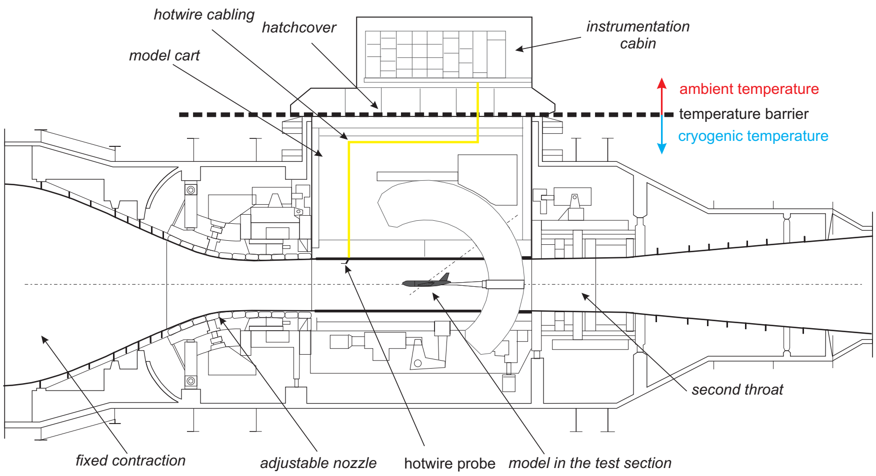

Fig. 6. ETW side view with model cart

The used hotwire probe is a Dantec miniature x-wire probe (Fig. 1 right). To increase the survivability of the wires, the original wires were replaced by 5 μm] thin gold-plated tungsten wires with a little slack between the prongs to compensate the shrinking during the tunnel cooldowns. The two wires of the x-wire probe form an angle of 90 deg with each another and are inclined by 45 deg to the mean flow direction (Fig. 7), so that they are capable to measure two-dimensional insteady flow fields. Because of the new wire material a test over the complete temperature range has been performed in a cryo chamber to measure the change of wire resistance with temperature. To compensate for resistance changes due to temperature within the probe body and the prongs a double shortcut probe (Fig. 1 left) is used.

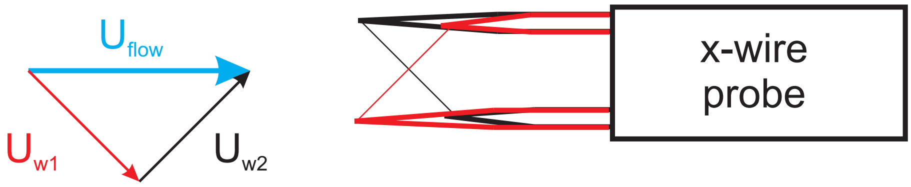

Fig. 7. x-wire probe layout and used velocity definition

The used anemometer system is a Dantec StreamLine Research Constant Temperature Anemometer system with two installed anemometer units operated in a symmetrical 1:1 bridge configuration. This configuration is needed because a of the long cables and the described necessity to compensate their resistance. To adjust the overheat ratio of the hotwires, external precision potentiometers were used. The resulting bridge layout is presented in Fig. 8

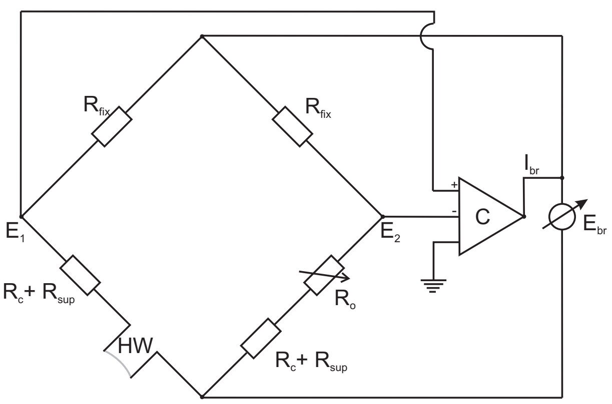

Fig. 8. Anemometer bridge layout

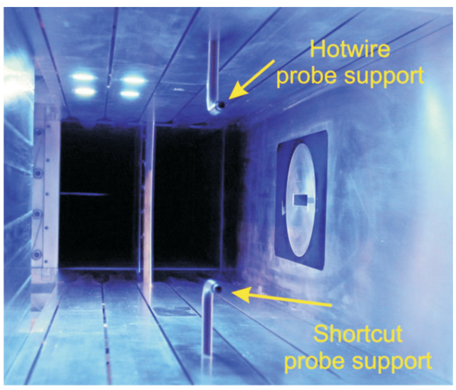

Fig. 9. PETW probe installation

The Dantec anemometer is connected to a high speed data acquisition system, recording the DC and AC compo-

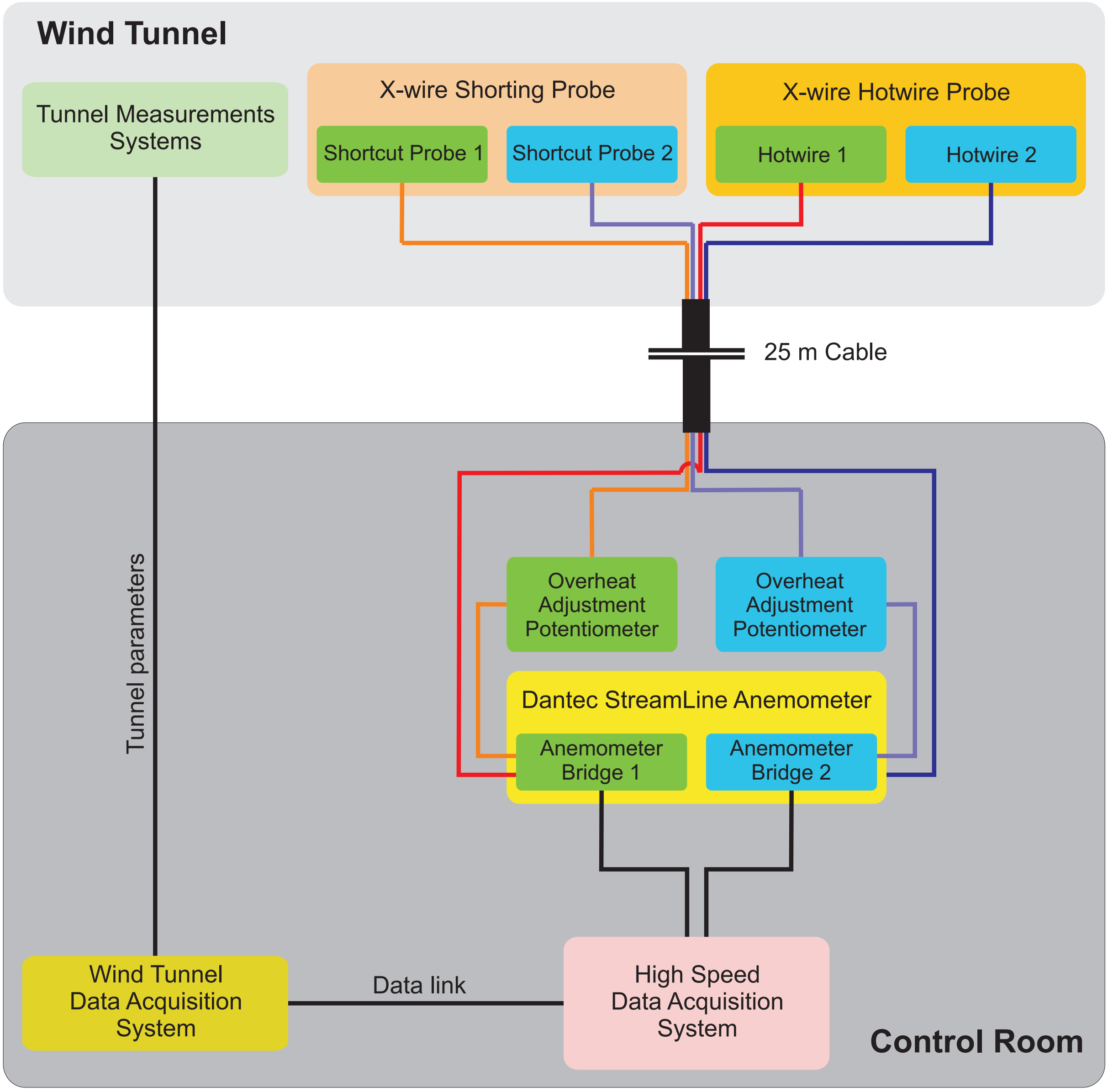

Fig. 10. Hotwire setup

nents of the two hotwires with 100 kHz and being connected to the tunnel data acquisition monitoring the tunnel flow parameters and temperatures. The complete setup is displayed in Fig. 10.

This setup was identically used in PETW to get there representative results for predicting ETW's behavior. Even the 25 meter cable was also used in PETW with a representative length of warm and cold part as in the ETW setup. The 2-wire probe was installed at the center of the top wall outside the boundary layer, while the compensating shortcut probe was mounted mirrored on the bottom wall. Fig. 9 shows the installed probe supports in the PETW test section.

V. Results

A. Steady Results

Velocity

Before using the hotwire measurement technique to assess the wind tunnel's turbulence level, it is necessary to understand the dependency of the anemometer output signal from the different flow parameters. Therefore the static output signal was measured under different flow conditions. In a first step the hotwire probes were calibrated over a wide velocity range using the DANTEC calibration unit. Because of the 45 [deg] inclination between the main flow direction and the wire only the velocity part perpendicular to the wire was used for the following presentations of the results, using the following relation:

$$U = \frac{\sqrt{2}}{2} \cdot U_{flow} \tag{19}$$

The results of such a calibration are shown in Fig. 11, representing a monotonically increasing calibration curve, resulting in an unique correlation between hotwire output signal and flow velocity according to King's law (Fig. 11). It has to be pointed out that using the DANTEC device implies a constant static pressure at the wire, while the total pressure has to be increased for generating higher speeds.

The next step was a repeat of this calibration under ambient temperature conditions in PETW by varying the Mach number at constant total pressure and temperature. This test leads at first glance to a complete different behavior of the output signal over velocity. At high velocities there is no longer an unique correlation between sensor signal and velocity (Fig. 12). The differences between the two calibrations are caused by the different measurement setups and consequently varying flow parameters. The DANTEC calibration unit was used at ambient air conditions with an open jet flow resulting in a **constant static pressure** for all velocities. In opposite, in PETW the total pressure is typically kept constant for a Mach number increase and therewith the also density is dropping down. With increasing Mach number the static pressure and the density are following the isentropic behavior at a **constant total pressure**. Fig. 13 compares the density characteristics for the two different set-ups, clearly demonstrating this effect. This first result pointed out, that for a hotwire calibration over velocity the standard PETW control with constant total pressures has to be changed to a constant static pressure control. It also verifies, that the density has a big influence on the hotwire's heat transfer. Nevertheless, it is possible to compare the two calibration by using the mass flow as reference. Fig. 14 shows the both matching calibration curves. Only at high speeds the PETW curve shows a slightly different characteristic, requiring further investigations.

To get a better understanding of the influence parameters on the hotwire signal and to separate them, an extensive test program over the complete ETW/PETW envelope was performed. By changing only one variable per time while keeping all other parameters constant it was possible to get the different influences clearly separated. Fig. 15 shows the measured test points as function of total temperature and density, while Fig. 16 shows the test points within the envelope of ETW and PETW. In addition at some test points the overheat ratio γ was varied.
The complete test program was performed twice, on one hand to check the survivability of the hotwire probe and on the other hand to check the repeatability of the measurements and therewith to get information about the uncertainty of the results. While the survivability of the probe can be stated as excellent, because both wires of the hotwire probe were not damaged during the complete testing, the uncertainty analysis is still ongoing and will be presented at a later stage.

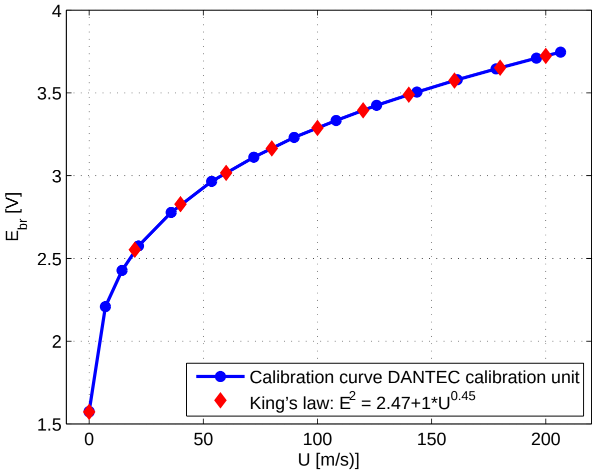

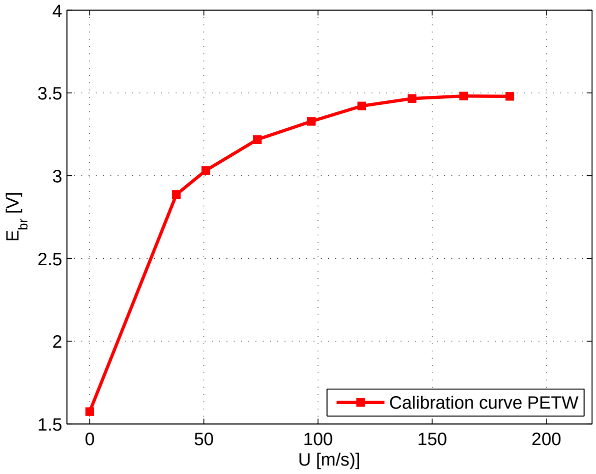

Fig. 11. Calibration results DANTEC calibration unit

Fig. 12. Calibration results PETW

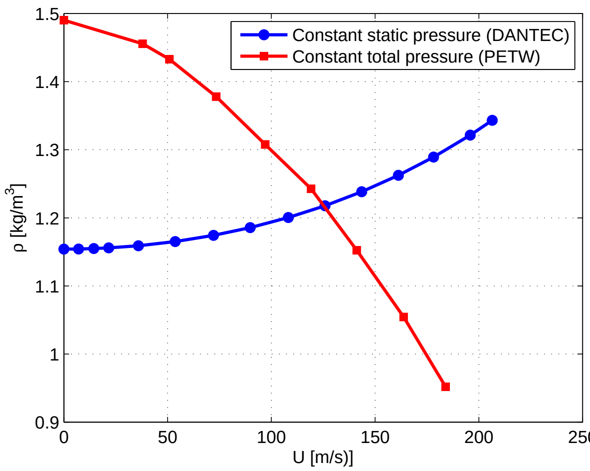

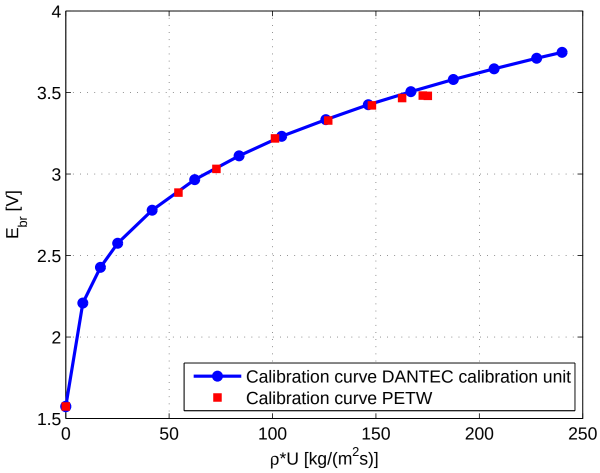

Fig. 13. Comparison of density characteristics over velocity

Fig. 14. Comparison of bridge output over mass flow

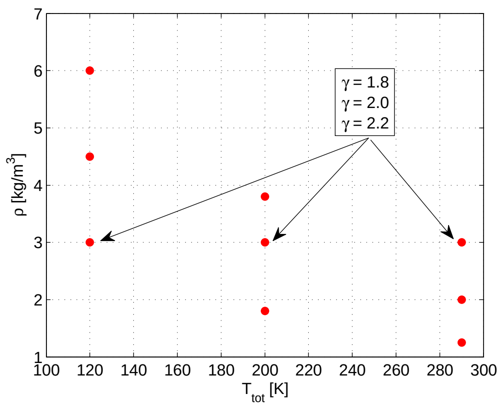

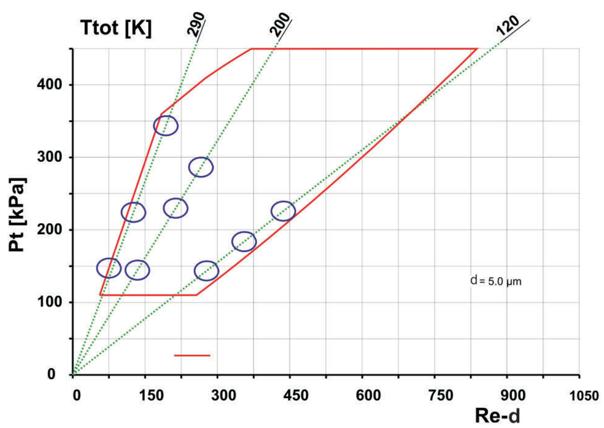

Fig. 15. Test points as function of temperature and density

Fig. 16. Test points within the ETW/PETW envelope

Density

The density was the first parameter investigated. Therefore, density was kept constant for the generation of different Mach numbers by controlling the static pressure. At each temperature level three different densities were generated. The Figures 17, 19 and 21 show the results of the density variations for the three different temperature levels. For all temperature levels it is obvious that the bridge output voltage reveals raised by increasing density. This may be due to an enlarged heat transfer from the wire to the surrounding flow, while the anemometer requires a higher current to keep the temperature constant when rising bridge voltage. The density influence is independent on the temperature level, allowing the finding of a correction to match the results for different density levels. For the gathered data a density of $\rho = 2.95[\mathrm{kg/m^3}]$ was chosen as reference for correction. The bridge output voltage of the other density levels could be matched to the reference by the following correction factor, independent of the temperature level as shown in Figure 18, 20 and 22:

$$E_{br_{corr}} = E_{br} \cdot (\frac{\rho_{ref}}{\rho})^{0.23} \tag{20}$$

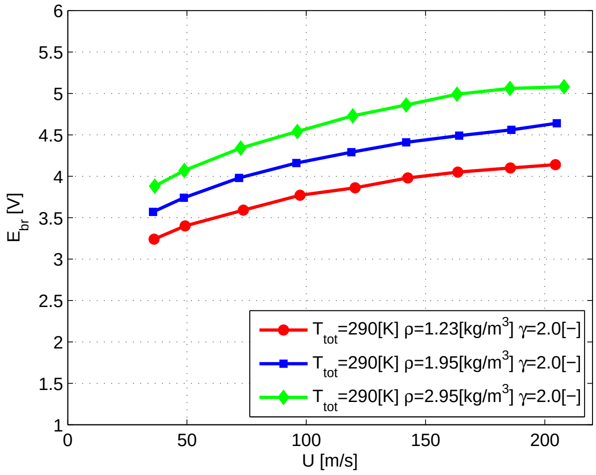

Fig. 17. Density influence at $\mathbf{T_{tot} = 290[K]}$

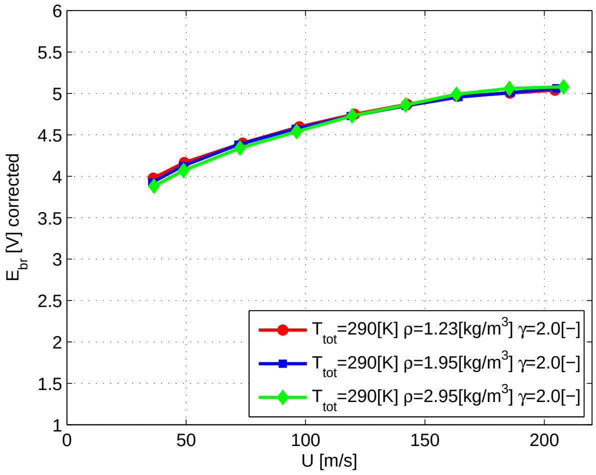

Fig. 18. Density influence at $\mathbf{T_{tot} = 290[K]}$ corrected

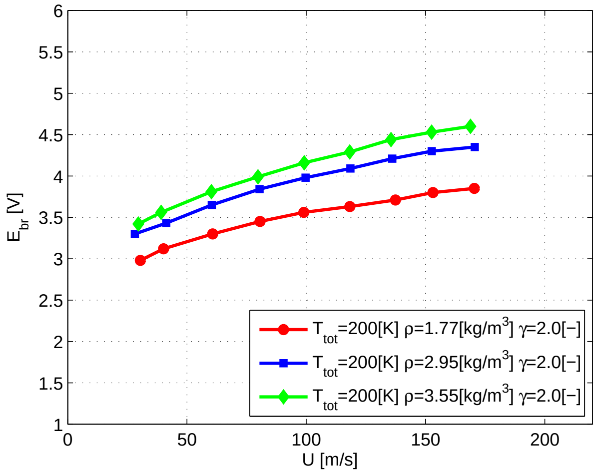

Fig. 19. Density influence at $\mathbf{T_{tot} = 200[K]}$

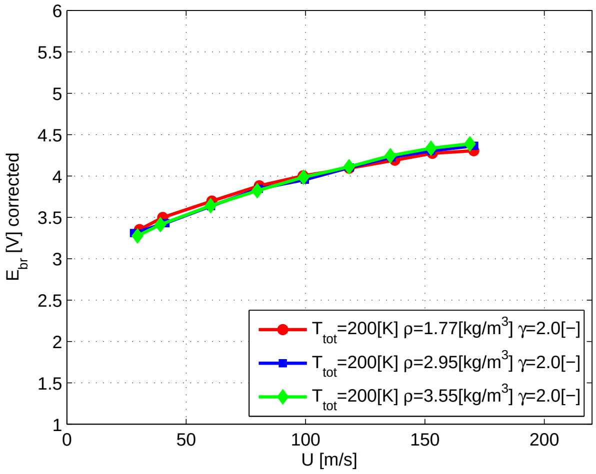

Fig. 20. Density influence at $\mathbf{T_{tot} = 200[K]}$ corrected

Overheat ratio

By changing the overheat ratio γ the wire temperature is changed and therewith also the heat transfer. Following equation 5 a higher wire temperature causes a bigger heat loss caused by the forced convection. This results according to equations 4 and 1 in an increase of the bridge voltage. The figures 23, 25 and 27 show this effect

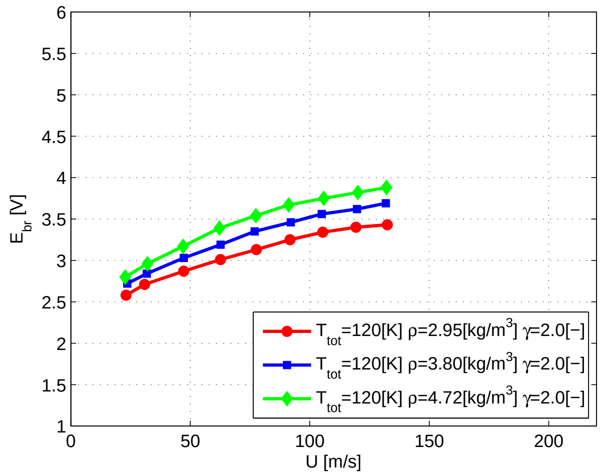

Fig. 21. Density influence at $\mathbf{T_{tot} = 120[K]}$

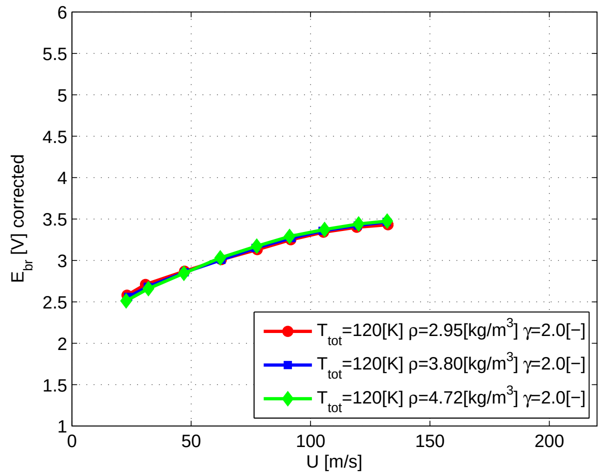

Fig. 22. Density influence at $\mathbf{T_{tot} = 120[K]}$ corrected

for three different overheat ratios at the tested three different temperature levels. It is obvious, that a change in overheat ratio has a similar effect on the bridge voltage at each temperature level. Therefore the application of a general correction factor to compensate for various overheat ratios can be extracted. Using $\gamma = 2.0[-]$ as the reference overheat ratio, the correction factor was evaluated as:

$$E_{br_{corr}} = E_{br} \cdot (\frac{\gamma_{ref}}{\gamma})^{0.6} = E_{br} \cdot (\frac{R_{w_{ref}}}{R_w})^{0.6} = E_{br} \cdot (\frac{T_{w_{ref}}}{T_w})^{0.6} \tag{21}$$

The results of the applied correction are displayed in the figures 24, 26 and 28.

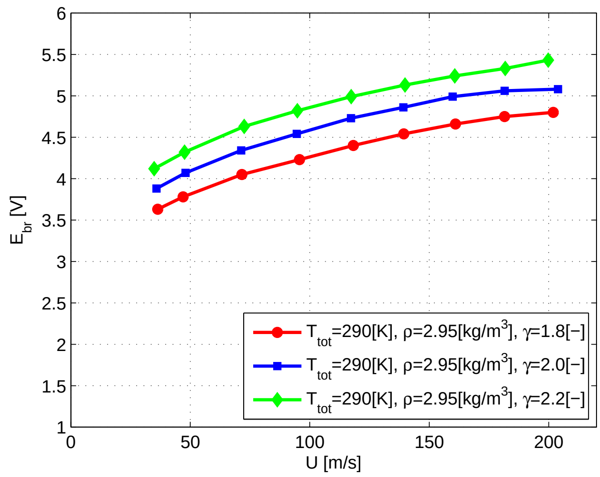

Fig. 23. Overheat ratio influence at $\mathbf{T_{tot} = 290[K]}$

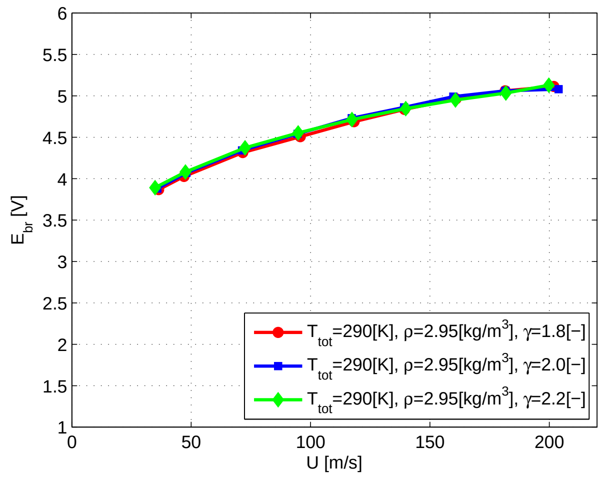

Fig. 24. Overheat ratio corrected $\mathbf{T_{tot} = 290[K]}$

Temperature

As shown above, the effects of density and overheat ratio are mainly independent of temperature, but the absolute level of the bridge voltage is decreasing with lower temperatures. The figures 29, 31 and 33 compare the bridge output voltages at constant density and overheat ratio for the three different test temperatures. The drop in bridge voltage with falling temperatures is not an effect of a different heat transfer at the wire, but is caused by the electrical anemometer setup. Assuming the anemometer uses a constant current to supply the bridge voltage is defined by:

$$E_{br} = (R_w + R_c + R_{sup} + R_{fix}) \cdot I_{br} \tag{22}$$

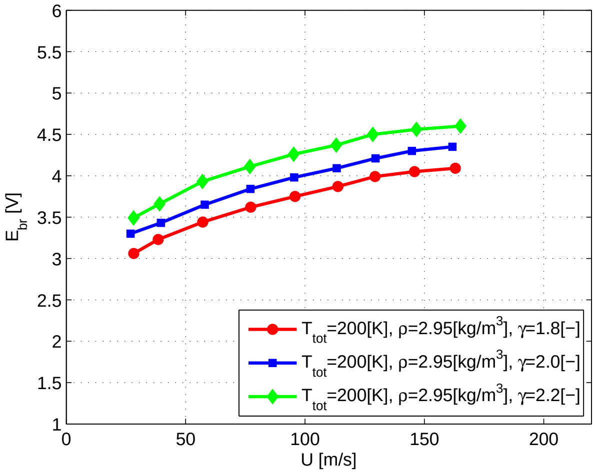

Fig. 25. Overheat ratio influence at $T_{tot} = 200[K]$

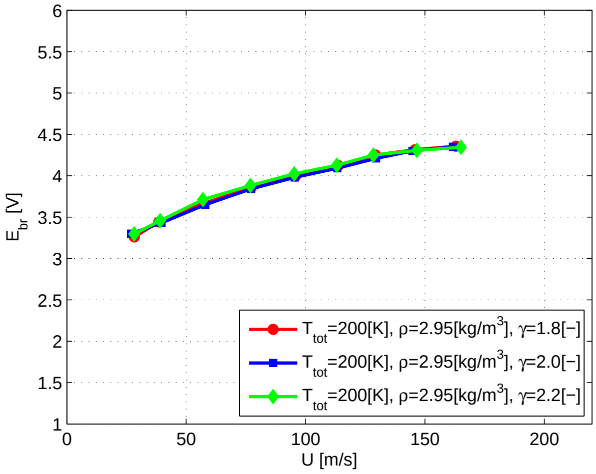

Fig. 26. Overheat ratio corrected $T_{tot} = 200[K]$

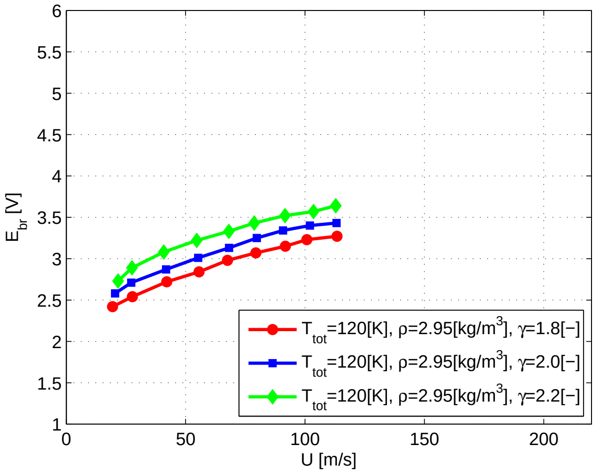

Fig. 27. Overheat ratio influence at $T_{tot} = 120[K]$

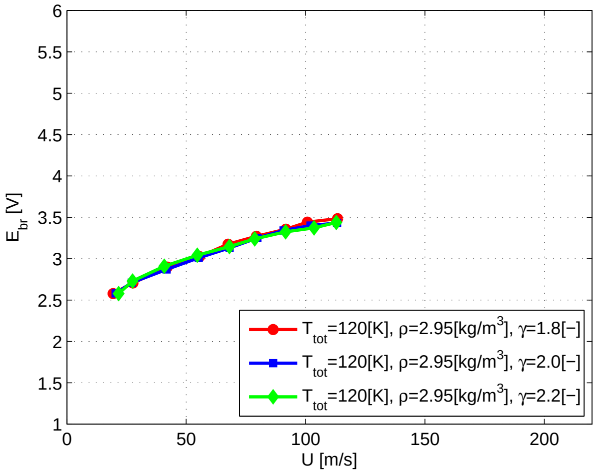

Fig. 28. Overheat ratio corrected $T_{tot} = 120[K]$

The linearly decrease of R_w, R_c and R_{sup} with temperature, results in a lower bridge voltage according to equation (22). Therefore, to analyze the pure temperature effect on the hotwire output, the bridge output has to be corrected for the different electrical bridge set-up first. Taking the ambient temperature as reference the correction may look like:

$$E_{br_{corr}} = E_{br} \cdot \frac{R_{w_{ref}} + R_{c_{ref}} + R_{sup_{ref}} + R_{fix}}{R_w + R_c + R_{sup} + R_{fix}} \tag{23}$$

Although theoretically simple, it is problematic to apply this correction due to the changing resistances. The wire resistance is changing directly with temperature because of the very low thermal mass of the wire and can be measured during the bridge setup. In contrast to that, it very difficult to determine the cable resistance. Because of the cable length and its warm and cold parts the cable resistance is changing over a long time period and from the operational view of ETW and PETW it is not possible to wait until the cable temperature is completely settled. Therefore the cable resistance was measured after a justifiable conditioning period during the bridge setup at the beginning of each temperature level. The results of the applied correction are shown in the figures 30, 32 and 34. The plots confirm that the cable resistance has a major influence on the correction. Looking at the curve for $\mathrm{T_{tot}} = 120[\mathrm{K}]$ shows the correction for $\gamma = 2.0[-]$ (Fig. 32) matching much better than for $\gamma = 1.8[-]$ (Fig. 30) and $\gamma = 2.2[-]$ (Fig. 34). This is due to the fact, that the $\gamma = 2.0[-]$ case was measured at the beginning of the test block at constant temperature and therewith shortly after measuring the cable resistance, while the over two overheat ratios were measured at the end of the run, where the cable resistance has likely changed.
Concluding, a direct temperature influence on the hotwire signal may not be extracted because of the uncertainties in the temperature correction. As an improvement for future application it may be mandatory to assess the line resistances ideally before each data capture.

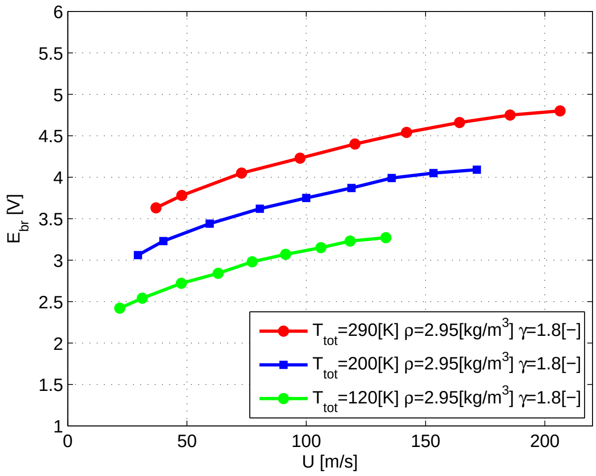

Fig. 29. Temperature influence at $\gamma = 1.8[-]$

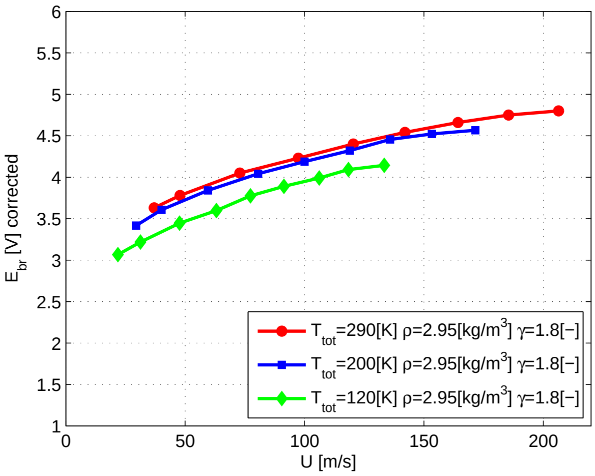

Fig. 30. Temperature influence at $\gamma = 1.8[-]$ corrected

Nusselt over Reynolds number

According to equation (10) the Nusselt number can be calculated based on the bridge voltage and some other parameters. Using the Nusselt number should allow to cancel out several influences to achieve one single calibration curve and to compare it to theoretical approaches. Applying equation (10) by using the problematic, but necessary correction of equation (23), the Nusselt number can be plotted as function of the wire Reynolds number.
The figures 35 and 36 give an overview about the overheat ratio and the density on Nusselt number. The plots clearly show that the calculation of the Nusselt number is not covering all influences on the hotwire. Especially the influence of the tunnel temperature is not compensated by the Nusselt number.
Looking at the results for the different overheat ratios in the figures 37, 39 and 41, some constant correction factors for all three overheat ratios can be found, achieving a fair match of all relevant graphs (Figures 38, 40 and 42). This documents the differences are not being caused by the overheat ratio and consequently not by wire characteristics. Applying the same correction factors to the different density runs, results in Fig. 44. Here the correction reduces the differences between the curves as well but does not compensate the different density influences.

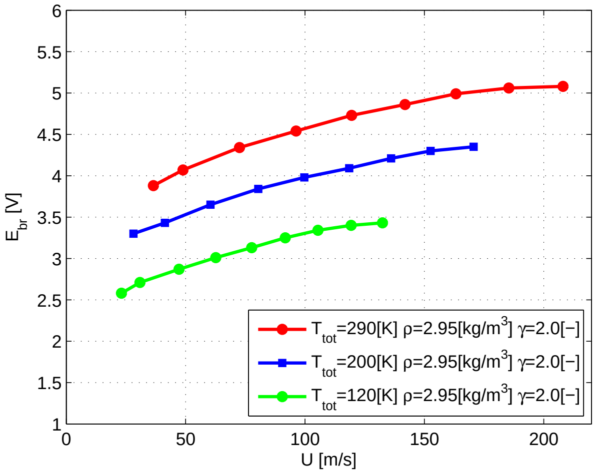

Fig. 31. Temperature influence at $\gamma = 2.0[-]$

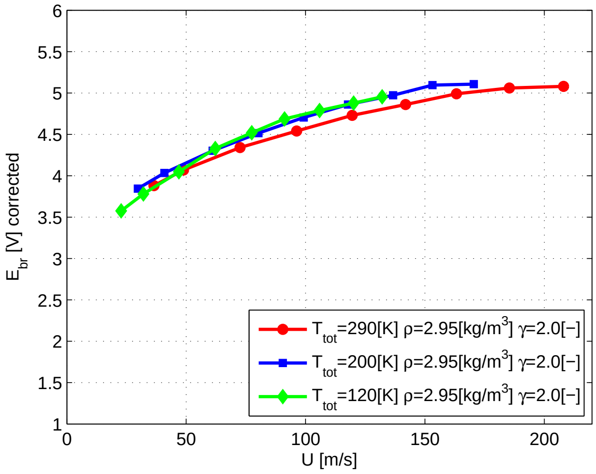

Fig. 32. Temperature influence at $\gamma = 2.0[-]$

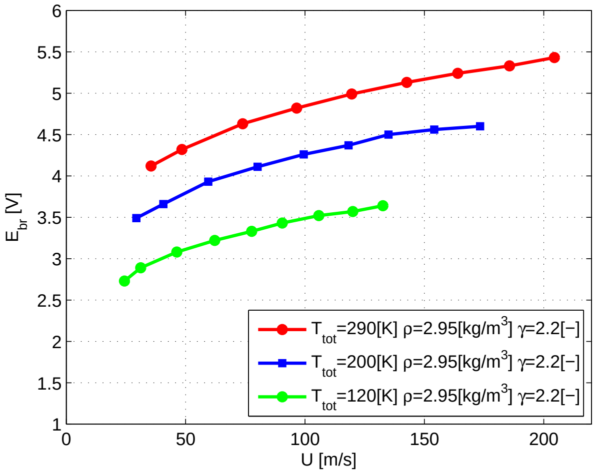

Fig. 33. Temperature influence at $\gamma = 2.2[-]$

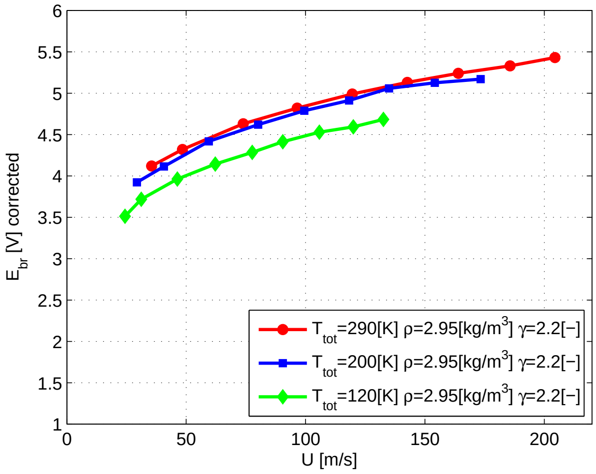

Fig. 34. Temperature influence at $\gamma = 2.2[-]$ corrected

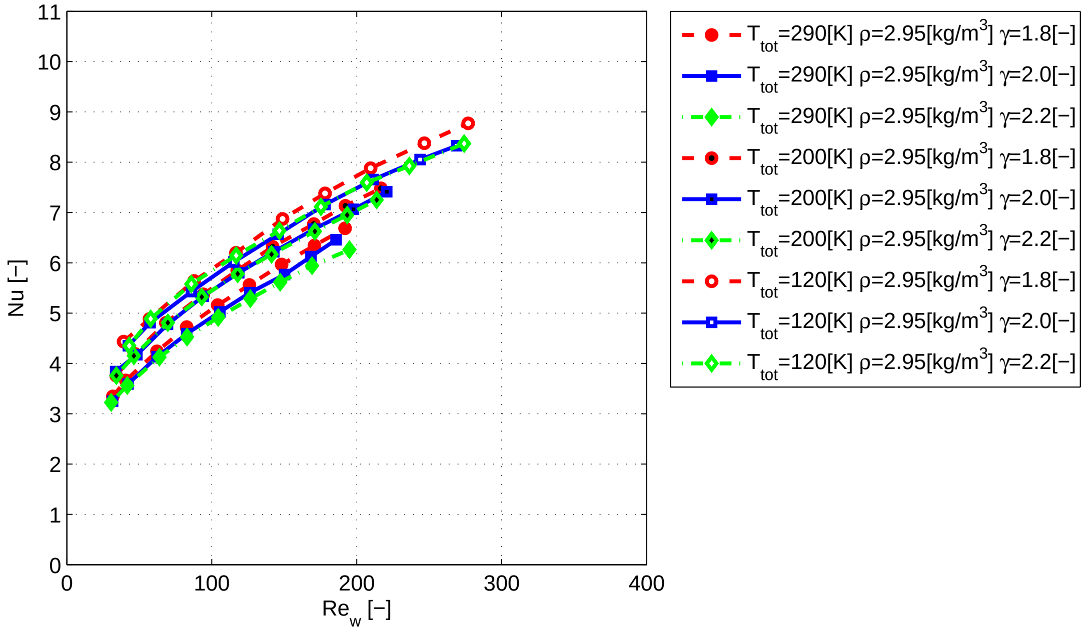

Fig. 35. Nusselt number over Reynolds number for different temperatures and overheat ratios

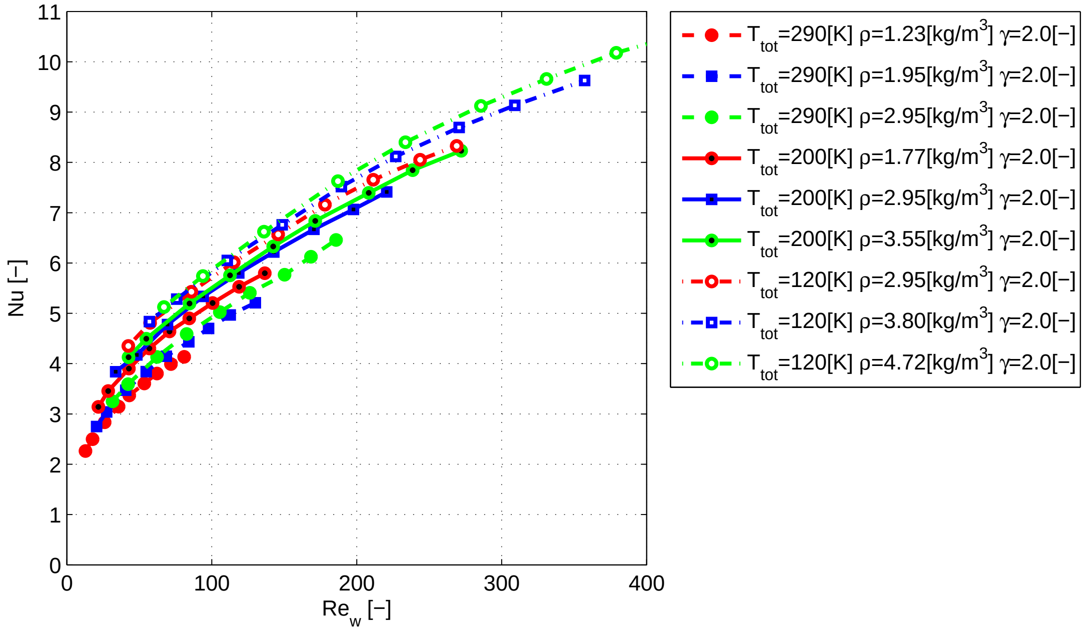

Fig. 36. Nusselt number over Reynolds number for different temperatures and densities

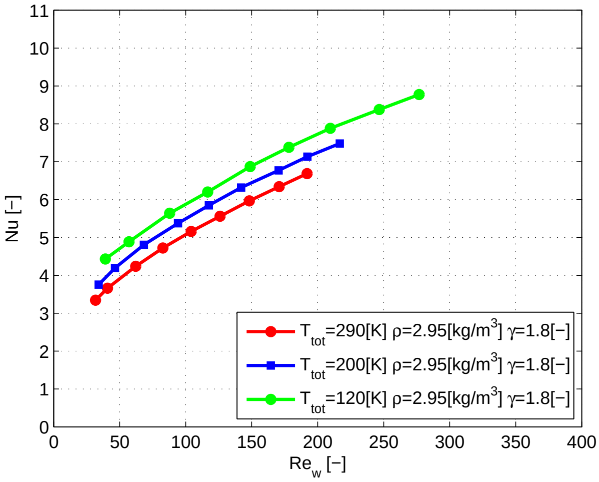

Fig. 37. Nusselt number at $\gamma = 1.8[-]$

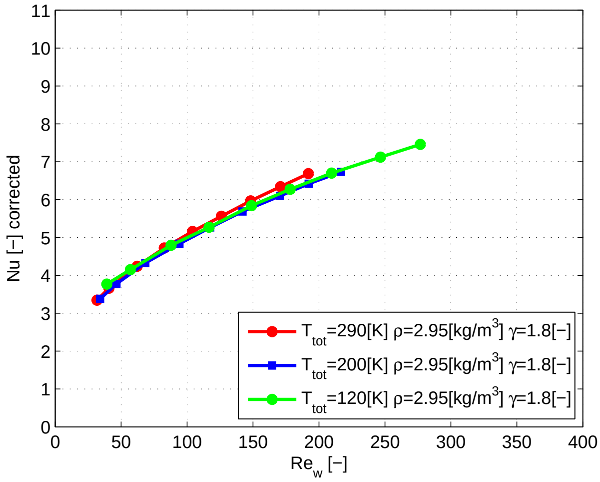

Fig. 38. Nusselt number at $\gamma = 1.8[-]$ corrected

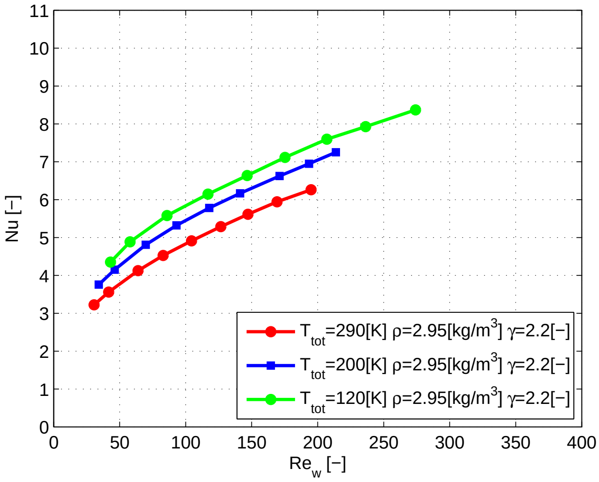

Fig. 39. Nusselt number at $\gamma = 2.0[-]$

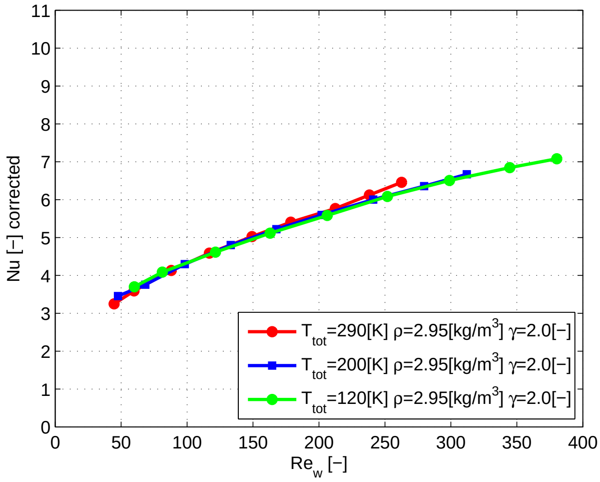

Fig. 40. Nusselt number at $\gamma = 2.0[-]$ corrected

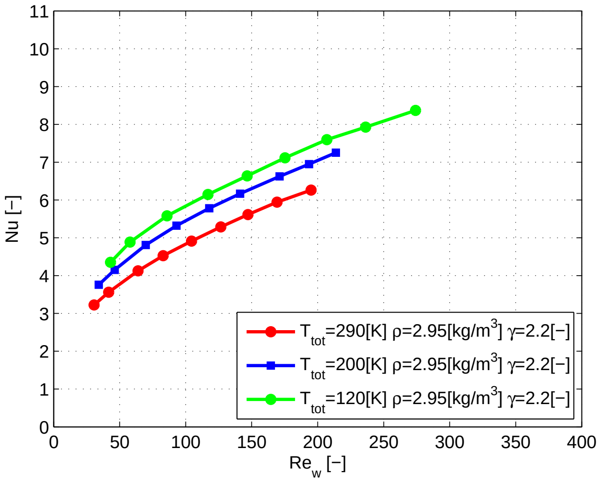

Fig. 41. Nusselt number at $\gamma = 2.2[-]$

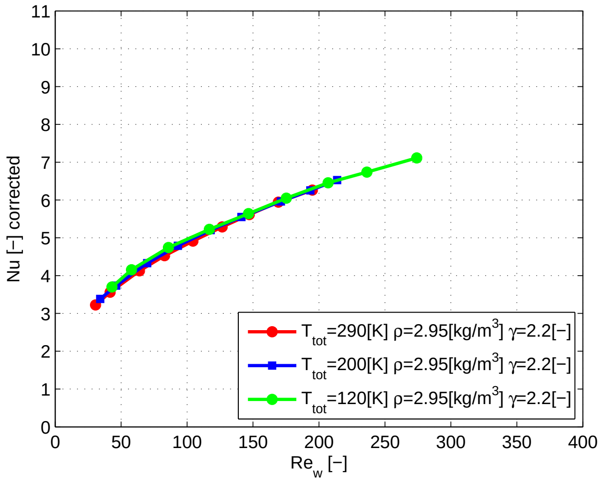

Fig. 42. Nusselt number at $\gamma = 2.2[-]$ corrected

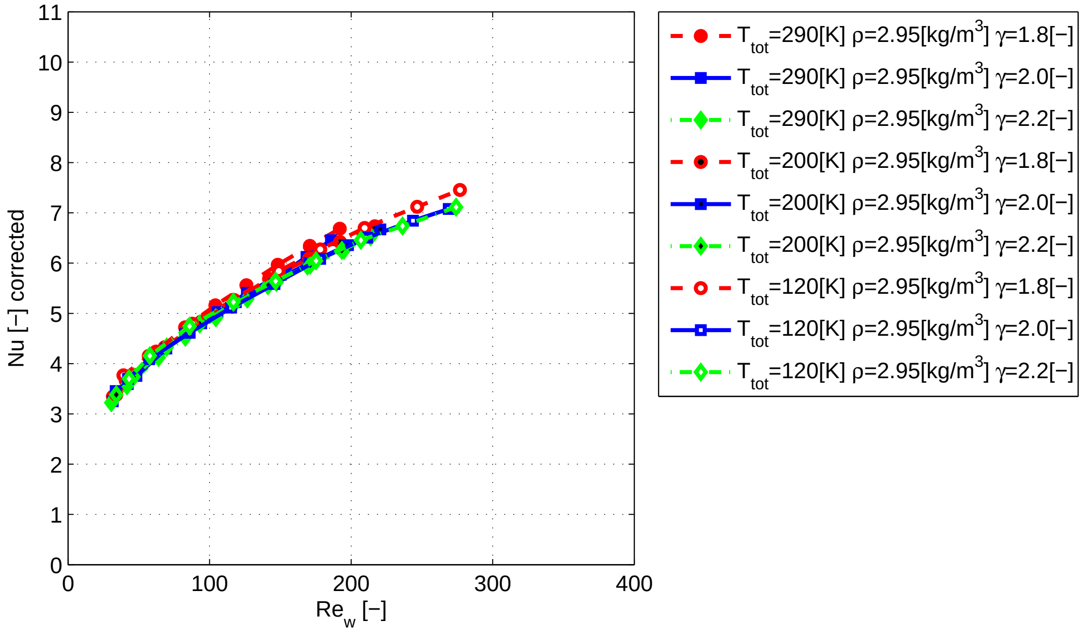

Fig. 43. Nusselt number over Reynolds number for different temperatures and overheat ratios

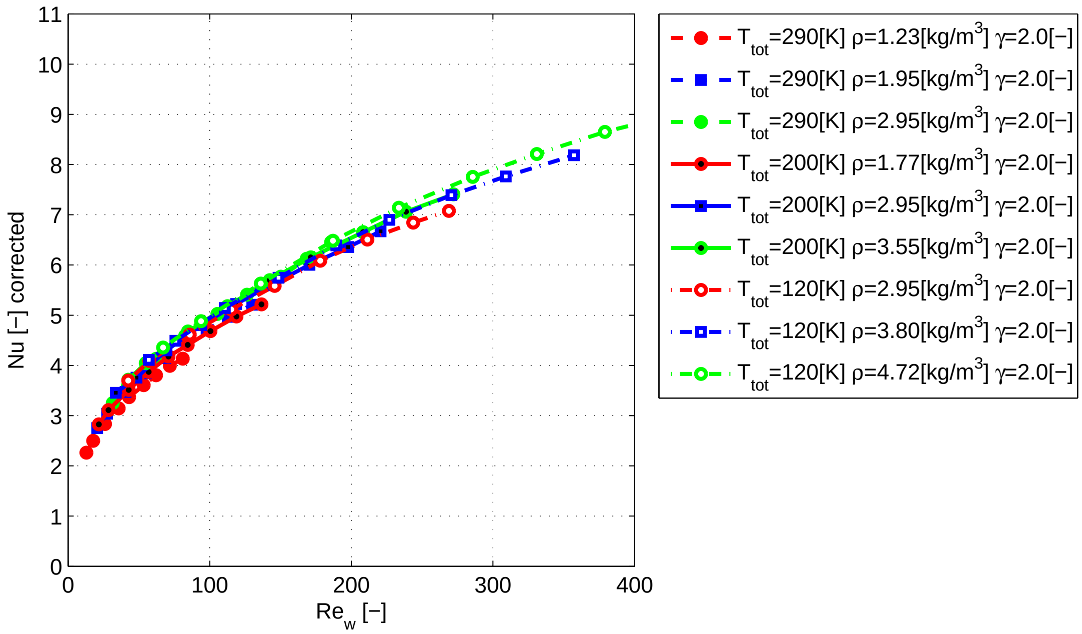

Fig. 44. Nusselt number over Reynolds number for different temperatures and densities

B. Unsteady Results

The amount of gathered unsteady data is tremendous, so the analysis and interpretation of these data is still ongoing and therefore no final conclusion can be extracted yet. To avoid misleading conclusions based on not comprehensively analyzed data, the presentation of results for turbulence levels is postponed to a follow on paper, which will focus on the unsteady results in detail. Nevertheless, some obtained spectra are given exemplarily below. Figures 45 to 48 present the power spectral density as function of the frequency up to 40 kHz. These spectra should give a first impression of the different influence parameters discussed for the steady results and their impact on the unsteady results.

In the low frequency range (f<100Hz) an increase of the PSD with raising Mach number can be stated. For higher frequencies Mach number effects seem to be pretty small except M=0.2 (Figure 45).

Varying density at constant Mach and temperature reflects little effect on the spectrum (Figure 46). Note that blade passing frequencies are ranging from 1000 to 7000Hz.

Figure 47 documents a diminishing effect of the overheat ratio on the spectra, here shown for M=0.7 at 120K and low tunnel pressure.

Finally, Figure 48 presents the spectra obtained at constant density and Mach number under variation of the tunnel temperature. These conditions can only be achieved by variation of the total pressure in the tunnel. Some shifted peaks in the frequency range 1000 to 10000Hz can be identified eventually based on the temperature relevant change of the speed of sound.

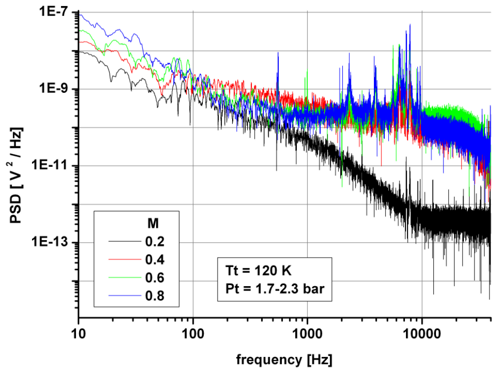

Fig. 45. Frequency spectra for varying Mach numbers

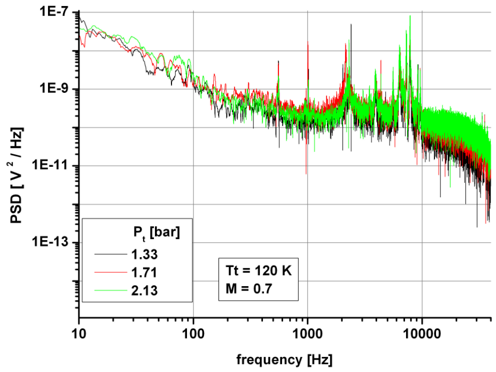

Fig. 46. Frequency spectra for varying density

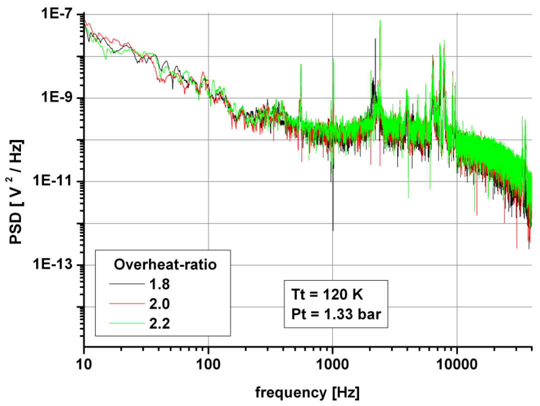

Fig. 47. Frequency spectra for varying overheat ratio

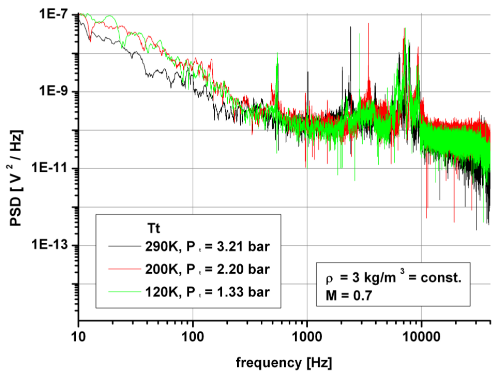

Fig. 48. Frequency spectra for varying temperature

VI. Conclusion

The paper presents the achieved results of hotwire measurements under cryogenic conditions in the pilot facility PETW of the European Transonic Windtunnel. The facility is establishing this measurement technique to support flow quality assessments required by future testimg of laminar wings.
To validate this for an application in a cryogenic environment an extensive test program with varying test parameters over the complete operational range of ETW/PETW was performed and lead to a unique database of hotwire results. The results obtained by the experimental investigations verified the general applicability of the measurement technique under the given conditions, by showing an excellent survivability of the hotwire probe on the one hand and providing a consistent data set on the other hand.
The paper focuses on the basic discussion about the different influence parameters on the hotwire. The understanding of these parameters, namely velocity, density, temperature and overheat ratio is essential for the analysis of hotwire data with respect to turbulence measurements. By varying only one parameter per time, the influences could be clearly separated. It may be concluded their influence to exist on the heat transfer as well as on the general bridge setup of the anemometer. Influences on the heat transfer could be successfully matched to reference values by using correction terms, while the compensation of a changing bridge setup is more challenging, due to the difficulty in measuring the thermal-floating resistances of the cable and the probe support during hotwire operation.
Summarizing, the hotwire measurement technique is applicable under cryogenic condition from the low to the high speed range and will provide reasonable results. Several parameters influencing the steady hotwire output could be identified, leading to demanding interpretations. Hence, with respect to the complexity of the subject and the amount of gathered data no conclusion could be made regarding the influencing effects on the unsteady data so far. The outcome of further ongoing analysis is supposed leading to the turbulence level of ETW and PETW. The results of these further investigations are considered to be published in a future paper.

References

[1] Archambaud, J.P., *Howire and Pressure Probe Measurements of flow fluctuations in ETW during the Pathfinder Campaign*, ONERA, TELFONA Project D3.1-2b, 2009

[2] Jorgensen F.E., *How to measure turbulence with hot-wire anemometers - a practical guide*, Dantec Dynamics, 2002

[3] Godden, J.H.M., *Turbulence Measurements in the Cryogenic DNW-KKK Wind Tunnel*, CEAS 2009 European Air and Space Conference, Manchester, 26. - 29. October 2009

[4] Horstmann C.C.; Rose W.C., *Hot-Wire Anemometry In Transonic Flow*, NASA TM X-62,495, 1975

[5] King, L.V., *On the Convection of Heat from Small Cylinders in a Stream of Fluid*, Phil. Trans. of Toy. Soc., Ser.A. Vol. 214, No. 14, p. 373-432, 1914

[6] Michel, U., *Combined Hotwire - Hotfilm Measurements in cryogenic Environment in the PETW*, DLR Institute of Propulsion Technology, Private communication, 1994

[7] Michel U., *Experimental assessment of unsteady flow quantities in wind tunnels with hot-wire anemometry*, DLR Institute of Propulsion Technology, Berlin, 2004

[8] Nitsche, W., *Strömungsmesstechnik*, Springer Publication Heidelberg, 1994